INTERACTIVE CONTROL ENGINEERING
Principles and Applications

Volume 20 Motion Control, Robotics, and Autonomous Systems

CHAPTER 13

Robotic Peg-in-Hole Simulator for Compliance, Jamming and Force Control Through Contact

Pages 306–328

Edited by John D. Hedengren

How to cite this chapter. "Robotic Peg-in-Hole Simulator for Compliance, Jamming and Force Control Through Contact," in *Motion Control, Robotics, and Autonomous Systems*, John D. Hedengren, Ed., vol. 20 of *Interactive Control Engineering: Principles and Applications*. Advanced Process Solutions, LLC, 2026, ch. 13, pp. 306–328.

The page numbers in this file are those of the printed volume.

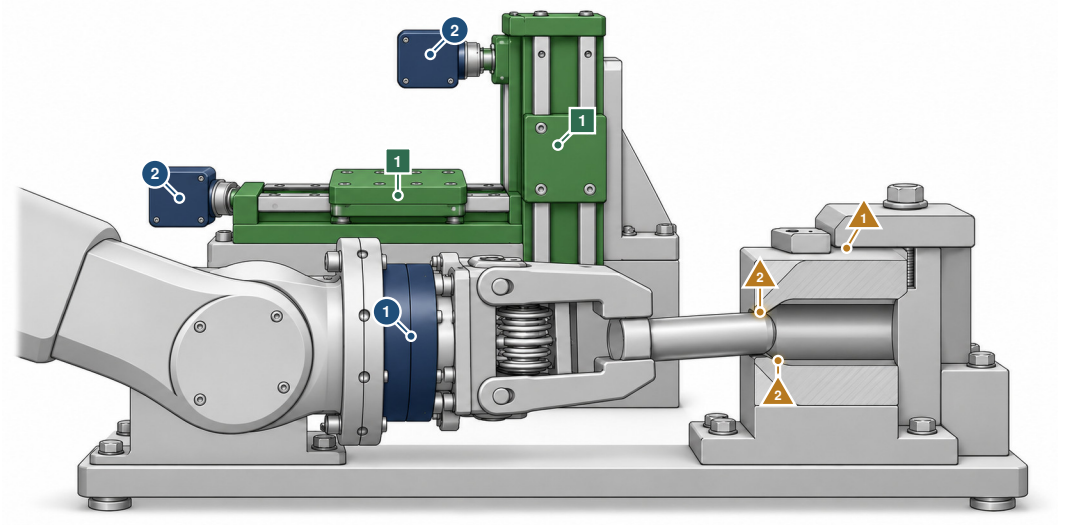
The app for this chapter
https://apmonitor.com/apps/robot-force-assembly/

The volume online: contents, other chapters and citation records
https://apmonitor.com/apps/books/v20-motion-robotics/#robot-force-assembly

Copyright © 2026 Advanced Process Solutions, LLC. All rights reserved. Produced by Advanced Process Solutions, LLC.

CHAPTER 13

Robotic Peg-in-Hole Simulator for Compliance, Jamming and Force Control Through Contact



The controller moves 1 robot axes that move the peg across and into the hole

The controller reads 1 wrist force sensor, read through a lag 2 position encoders on the axes

What disturbs it 1 fixture shifted or tilted from where the program aims 2 friction where the peg touches the hole

Notice the tilted peg touching the bore at two amber points, the two-point contact that can jam it, with the insertion drawn lying on its side. Illustration, not to scale.

IN PLAIN TERMS **Pushing a Peg Into a Hole**

The main idea. A robot arm puts a pin into a hole that is only a hair wider than the pin. Once the pin touches the part, the robot can no longer choose exactly where the pin goes, only how hard it pushes.

The challenge. A robot that holds its path very stiffly turns a tiny miss into a force large enough to break the part. A springy hold lets the hole guide the pin in. But a tilted pin can still wedge, and a late force reading can hide hard knocks.

Why it matters. Shafts, pins and connectors all go together this way, so these choices decide whether a part is made or scrapped.

THREE WAYS TO READ THIS CHAPTER

Explore	11 min	the first page, the fact on the first touch (Section 13.1), the history segment (Section 13.2), the try-it segments of cases 2 and 7 (Section 13.5), the fact on the hundred parts (Section 13.6) and the key points
Study	45 min	the whole chapter with its three pause points and the twelve exercises at its end
Practice	15 min	the first page, the measured cases (Section 13.6), Technology in Practice (Section 13.7), Limitations (Section 13.8) and the open challenges

The control question Once a peg touches its part, the part fixes some of the peg's coordinates and the controller can only decide how hard to push along them. How do stiffness, friction, landing speed and a late force signal each turn a position error of a few tenths of a millimeter into a contact force, a jam or a damaged part?

Learning objectives

- Compute the fixture offset a stiff position servo can absorb on a chamfer, from the chamfer force factor and the damage limit.
- Estimate the force of a landing from the effective mass of the contact corner and the approach speed.
- Predict with a moment balance the depth at which a tilted peg jams, and choose the rotational stiffness that frees it.
- Explain why the delay margin of the insertion force loop is set by the sensor lag and the filter, and why a calm force reading can hide a hammering press.
- Decide where a guarded move must slow down, and where the compliance center belongs.

Prerequisites Sections 1.4.8 (impedance, landing force and the delay of a force loop), 1.6.2 (velocity-form PID), 1.3 (loop action) and 1.6.4 (scenarios, scorecard and CSV file).

The app https://apmonitor.com/apps/robot-force-assembly/

See also Volume 7, Chapter 13 for a contact process whose stability boundary is set by a delay, and Volume 7, Chapter 4 for a force that friction caps at the contact patch.



13.1 Introduction

An industrial robot repeats a programmed path to a small fraction of a millimeter, which is enough for welding, painting and transfer, where nothing on the path pushes back. Assembly ends in contact instead. A shaft entering a bearing, a pin entering a connector and a cartridge entering a housing are versions of one task, a peg entering a hole whose clearance is small beside the uncertainty in where the hole is, because fixture tolerance, part variation and robot calibration all add to the position error [1, 2]. Once the peg touches the part, the part's surfaces fix some of the peg's coordinates, and along those directions the controller can prescribe only a force [3]. Hybrid position and force control assigns each task direction to one of the two, and impedance control prescribes the relation between them [4–6]. Section 1.4.8 sets out the impedance law, the landing force and the delay margin of a force loop in general. This chapter applies them to one peg.

The belief this simulator is meant to overturn is that a more precise position controller makes a better assembly robot. After contact, precision becomes force. The robot's own servo in the simulator holds the tip with 200 N/mm, so each micrometer by which the program and the part disagree costs 0.2 N. With the fixture shifted 0.4 mm the servo damages the part and the contact force climbs to 136.1 N, while a programmable spring of 3 N/mm puts the same peg into the same part with a largest contact force of 13.7 N. Stiffness is the rate of exchange between position error and force, and once the peg is in contact it is a design choice rather than a mark of quality.

The class of problem is general. A grinding wheel on a casting, a polishing pad under a regulated normal force, a friction stir tool plunged into a plate, the foot of a walking robot meeting the ground and a surgical instrument meeting tissue all pass from free motion, where position control is enough, into constrained motion, where force has to be controlled or at least bounded [2, 6]. Volume 9, Chapter 3 plunges such a tool under a force limit, and Chapter 14 closes a force loop on tissue. Three difficulties recur across the class, and a block diagram that treats the environment as a linear spring shows none of them. Geometry and friction can jam a part that more force will not free [1]. An impact is decided by the moving mass and the speed at contact [7], and in the simulator it is over within a millisecond, before any feedback can act. A force loop is bounded by the dynamics that lie between the actuator, the sensor and the environment [8, 9]. The simulator produces each difficulty on purpose

and draws the contact forces the controller never reads beside the lagged reading it does act on, so that a jam, an impact and a hammering press are measured rather than inferred.

> ✦ DID YOU KNOW? **The First Touch Is the Hardest**
>
> The force spike of the first impact between tool and part is often three to five times larger than the forces of the rest of an assembly [10]. In NIST tests of two arms stepping to a contact force, the overshoot stayed well under 10 N along the horizontal axes and was typically well over 100 N along the vertical one [11].

This chapter attaches a number to each of these difficulties, with a peg-in-hole simulator in which stiffness, friction, landing speed and sensing can each be changed alone and their consequence read as a contact force, a jam or a damaged part. Impedance control, force loops closed around a position reference and quasi-static jamming analysis each have a long record [1, 5, 12], and the chapter uses them as established methods. Section 13.2 traces force control in assembly. Section 13.3 sets down a planar contact model with six penalty sites and a friction law that holds a stuck contact without creep, with every relation and constant needed to rebuild it. Section 13.4 gives the three controllers, which read only a lagged, noisy and optionally delayed wrist sensor. Section 13.5 checks four short estimates against the nonlinear simulator, for the offset at which the stiff servo damages the part, for the force of a landing, for the depth at which a jammed peg stops and for the delay a force loop can tolerate. Section 13.6 measures the eight cases and the challenge, in which each failure is met on its own. Section 13.7 names the devices of real assembly cells, Section 13.8 states the limitations, Section 13.9 draws the results together, and the exercises of Section 13.10 work through the cases.

13.2 Force Control and Compliant Assembly

Automated mechanical assembly was studied in the 1970s as a problem of using force and position information together while parts are in contact. The history segment below follows its first two answers, force feedback and the passive remote center compliance.

> ⧖ HISTORY **Two Answers to the Peg, 1977 and 1982**
>
> In the 1970s, automating mechanical assembly meant using force and position information together while parts touched. One answer, published in 1977, used force and position sensors to make small corrections in the paths of parts in contact. It showed that such force feedback strategies must be posed as control problems, with stability bounds derived from simple linear actuator models and sampled-data control [8]. The other answer was passive. A quasi-static analysis of 1982 set out the geometric and force equilibrium conditions for mating rigid parts, explained the action of the remote center compliance and gave guidelines for choosing its parameters [1]. Such a device lets the held part give way to forces and torques, so that it adjusts to small lateral and angular errors [10].

Programmable compliance followed within a few years. A formal account of compliant motion separated the constraints that the task geometry imposes from those the controller remains free to choose [3]. Hybrid position and force control combined readings from a force-sensing wrist with joint positions to meet position and force trajectories in a coordinate system tied to the task [4]. Impedance control then argued that control of position or of force alone is inadequate once a manipulator is coupled to its environment, and that a manipulator handling inertial objects must behave as an impedance [5]. A review in 1987 traced these lines, compared the impedance and hybrid strategies built on them, and discussed the stability problem they share [2], while dynamic models of the robot, the sensor and the environment were introduced to explain where that problem comes from [9].

A second arrangement closes the force loops outside the robot's own position control. The position loops decouple and linearize the arm and present the external controller with a plant that is easy to model, and the effect of a passive compliance on task speed and disturbance rejection was analyzed in the same framework [12]. Explicit force control strategies were then compared in theory and

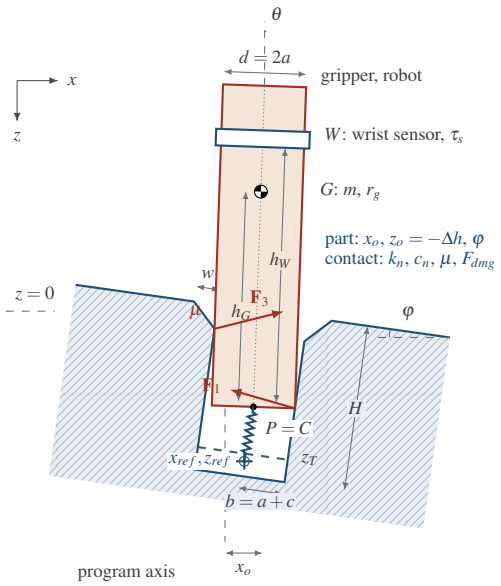


Figure 13.1 Section through the peg and the chamfered hole, drawn in two-point contact and not to scale. The part sits at offset x_o, height $z_o = -\Delta h$ and tilt φ from the program's nominal hole, and its fixture frame (X, Z) has its origin at the hole's top center. The peg of width $d = 2a$ leans θ from the vertical, its tip P coincides with the compliance center C at the default $h_C = 0$, and G and the wrist sensor W lie h_G and h_W above it. The impedance spring pulls C toward the reference (x_{ref}, z_{ref}), and the contact forces $\mathbf{F}_1$ at the right corner and $\mathbf{F}_3$ at the left entry edge carry friction μ. The hole of half-width $b = a + c$ has a chamfer of width w, depth H and the target depth z_T.

in experiment [13]. When the position error exceeds what a chamfer can capture, the hole has to be found before it can be entered, and search strategies for peg-in-hole assembly under position uncertainty address that case [14]. Two later threads frame the damage limit and the landing speed of this simulator. Robots that work beside people made the force of an unintended impact a safety requirement, measured with automotive crash-test methods on a lightweight arm [7], a budget that Chapter 15 keeps beside a person, and the force control capability of robots is now benchmarked by experiment [11].

13.3 Peg, Part and Contact Model

The simulated cell is a vertical section through a peg 12 mm wide held by the robot above a part with a chamfered hole, as shown in Figure 13.1. The hole leaves 50 µm of clearance on each side, its mouth carries a 45° chamfer 0.8 mm wide, it is 14 mm deep, and the insertion is complete at 10 mm. The wrist, the gripper and the peg move as one rigid body of 2 kg whose center of mass G lies 90 mm above the peg tip P. The part sits in a fixture whose pose the controller does not know, made of a lateral offset x_o, a tilt φ about the hole's top center and a height error Δh, while the program aims at a nominal hole at $x = 0$ with its top face at $z = 0$. The model is written in SI units and displayed in millimeters, micrometers and degrees.

Table 13.1 classifies the variables. Fifteen states are integrated, the position x_G, z_G and tilt θ of the center of mass and their rates v_x, v_z, ω, one tangential friction spring b_i at each of six contact sites, and three lagged components of the wrist sensor reading. The depth coordinate z points down into the hole, and θ is positive when the top of the peg leans toward $+x$.

Table 13.1 Variables, With Nominal Values of the Default Cell

Symbol	Role	Nominal	Range
F_{ins}	CV, insertion force reading	SP 12 N	SP 2–40
F_x	CV, side force reading	SP 0 N	SP ± 10
z_{ref}	MV, z command	path	-5 to 13 mm
x_{ref}	MV, x command	0 mm	± 3 mm
F_{cx}, F_{cz}, M_c	wrench at C	—	± 300 N, ± 20 N m
x_o	DV, fixture offset	0 mm	± 2
φ	DV, fixture tilt	0°	± 3
μ	DV, friction coefficient	0.20	0.05–0.8
Δh	DV, part height error	0 mm	-1 to 2.4
x_G, z_G, θ	states, pose of G	tip 3 mm up	—
v_x, v_z, ω	states, rates	0	—
$b_0 \ldots b_5$	states, friction springs	0	$k_t \lvert b_i \rvert \le \mu F_{n,i}$
$F_{s,x}, F_{s,z}, M_s$	states, lagged sensor	0	—
Z	output, true depth	—	target 10 mm
$\max_i \lvert \mathbf{F}_i \rvert$	output, largest contact	—	damage > 60 N

13.3.1 Rigid Body

The end effector obeys the Newton-Euler equations written at G, where the inertia is diagonal, as shown in Equation (13.1).

$$\begin{aligned} m\dot{v}_x &= F_{cx} + \textstyle\sum_i F_{ix} \\ m\dot{v}_z &= F_{cz} + mg + \textstyle\sum_i F_{iz} \\ mr_g^2\,\dot{\omega} &= M_c + (h_C - h_G)\,(F_{cz}\sin\theta + F_{cx}\cos\theta) \\ &\quad + \textstyle\sum_i \left[(p_{ix} - x_G)F_{iz} - (p_{iz} - z_G)F_{ix}\right] \end{aligned} \tag{13.1}$$

where (F_{cx}, F_{cz}, M_c) is the wrench the controller applies at the compliance center C, a height h_C above the tip, held constant over each control period, $\mathbf{F}_i$ is the contact force at site i acting at $\mathbf{p}_i$, r_g is the radius of gyration about G and g is gravity. The unit vectors $\mathbf{u} = (\sin\theta, -\cos\theta)$ up the peg and $\mathbf{r} = (\cos\theta, \sin\theta)$ across it place the tip at $P = G - h_G\mathbf{u}$, so that $x = x_G - h_G\sin\theta$ and $z = z_G + h_G\cos\theta$. Because the center of mass sits high, a sideways force at the tip also turns the peg, and the tip presents an effective lateral mass of $m/(1 + h_G^2/r_g^2) = 0.47$ kg to a sudden push.

13.3.2 Contact Sites

The part's profile in the fixture frame is the top face, two 45° chamfers, two walls at $|X| = b = a + c$ and a bottom at $Z = H$, where $a = d/2$ is the peg's half-width and c the clearance per side. World points map into that frame through Equation (13.2).

$$\begin{aligned} X &= (x - x_o)\cos\varphi + (z - z_o)\sin\varphi \\ Z &= -(x - x_o)\sin\varphi + (z - z_o)\cos\varphi \end{aligned} \tag{13.2}$$

with $z_o = -\Delta h$, so that Z evaluated at the tip is the true insertion depth. Contact is evaluated at six sites. Sites 0 and 1 are the peg's bottom corners $P \mp a\mathbf{r}$, tested against the whole profile. Sites 2 to 5 are the part's convex edges, the tops of the chamfers at $X = \mp(b + w)$, $Z = 0$ and the entry edges at $X = \mp b$, $Z = w$, tested against the peg's bottom face and its two sides. At each site the penetration δ_i is the distance to the nearest surface, $\mathbf{n}_i$ is the unit normal along which the part pushes the peg, and $\mathbf{t}_i = (-n_{iz}, n_{ix})$ is the tangent. One-point contact, two-point contact and jamming are not flags. They are what the six sites do with the geometry and the friction.

13.3.3 Normal Force and Friction

The normal force is a unilateral spring and damper whose damping fades in over the first δ_r of penetration, as shown in Equation (13.3).

$$F_{n,i} = \max\Big(0,\ k_n\delta_i + c_n\dot{\delta}_i \min(1,\ \delta_i/\delta_r)\Big) \tag{13.3}$$

in which $\dot{\delta}_i$ is the rate at which the peg's material point closes on the surface along $\mathbf{n}_i$, $k_n = 5\,\mathrm{N/\mu m}$ lumps the local compliance of the part, the fixture and the peg, $c_n = 1500\,\mathrm{N\,s/m}$ and $\delta_r = 0.25\,\mu\mathrm{m}$. The maximum keeps the contact from pulling and the ramp keeps the force continuous at touchdown, two faults of a plain spring and dashpot that a damping term growing with penetration also removes [15, 16]. The ramp is a quarter of the 1 µm that a 5 N press penetrates.

Friction is an elastic-plastic Coulomb law, as shown in Equation (13.4).

$$\begin{aligned} &\dot{b}_i = v_{t,i}, \qquad F_{t,i} = -\mathrm{clamp}(k_t b_i + c_t v_{t,i},\ \pm\mu F_{n,i}) \\ &b_i \leftarrow \mathrm{clamp}(b_i,\ \pm\mu F_{n,i}/k_t) \quad \text{after each step} \end{aligned} \tag{13.4}$$

in which $v_{t,i}$ is the slip velocity along $\mathbf{t}_i$, $k_t = k_n/2$, $c_t = c_n/2$ and μ is one coefficient for sticking and sliding alike. The spring b_i is zero whenever its site is out of contact. A stuck site holds any tangential load below $\mu F_{n,i}$ without creeping, and a sliding one has its spring returned to the friction cone after every step. Representing true sticking is the known difficulty in simulating friction near zero velocity [17], and a tangential spring with a plastic limit belongs to the elastoplastic family of friction models [18]. A law regularized around zero slip would let a loaded contact creep, and a wedged peg would slowly ooze through instead of jamming. The contact forces sum to the wrench of Equation (13.1), and their moments are also taken about the sensor point W, a height h_W above the tip, and about the tip itself.

13.3.4 Wrist Sensor, Encoders and Damage

The wrist sensor is a first-order lag on the contact wrench at W, and the controller samples it through noise, an optional delay and its own filter, as shown in Equation (13.5).

$$\begin{aligned} \tau_s\,\dot{\mathbf{F}}_s &= \mathbf{F}_{con} - \mathbf{F}_s \\ \mathbf{F}_{meas}(t) &= \mathscr{L}_{\tau_f}[\mathbf{F}_s(t-\tau_d) + \mathbf{n}_F] \end{aligned} \tag{13.5}$$

where $\mathbf{F}_{con}$ is the contact wrench, $\tau_s = 2\,\mathrm{ms}$ stands for the sensor's bandwidth and its anti-aliasing filter, $\mathbf{n}_F$ is Gaussian noise of 0.15 N on each force and 0.003 N m on the moment, τ_d is a transport delay read from a ring buffer by linear interpolation, and $\mathscr{L}_{\tau_f}$ is the controller's first-order filter of $\tau_f = 3\,\mathrm{ms}$, stepped by the exact hold expression. The sensor is taken as perfectly tared, so it reports the contact wrench without the weight or the inertia of the gripper. The joint encoders give the tip's x and z with 0.5 µm of noise and θ with 5 µrad, and the controller forms rates from a first difference filtered at 0.5 ms. The controller never reads the contact forces or the fixture pose.

The part is damaged at the first physics step on which any single contact carries a resultant $\sqrt{F_n^2 + F_t^2}$ above $F_{dmg} = 60\,\mathrm{N}$. An attempt ends inserted when the controller has declared it done and the true depth is within 0.1 mm of the target, and otherwise damaged, stuck inside the hole, or missed when the peg never finds it. In the challenge a new part is loaded after each attempt, with its fixture offset and tilt drawn uniformly from an envelope. A fixture change takes effect only while the peg is clear of the part, with no site carrying load and the tip at least 0.3 mm above the surface.

13.3.5 Parameters and Numerics

The plant parameters are listed in Table 13.2. A fixed 0.1 ms fourth-order Runge-Kutta step of the engine of Section 1.6.1, the framework's h, integrates Equation (13.1) with the friction springs and the sensor lags, and the plastic update of Equation (13.4) and the damage check follow every step.

Table 13.2 Plant Parameters. Adjustable Ones Are Sliders in the Model Panel, Hidden Ones Are Never Displayed, Code Ones Are Fixed in the Program

Symbol	Meaning	Value	Class
m	wrist, gripper and peg	2.0 kg	adjustable
r_g	radius of gyration about G	50 mm	hidden
h_G, h_W	G and sensor above the tip	90, 110 mm	hidden
F_{max}	force limit at the tool	300 N	adjustable
M_{max}	moment limit at the tool	20 N m	hidden
d, L	peg width, length below gripper	12, 50 mm	hidden
c	clearance per side	50 µm	adjustable
w	chamfer width at 45°	0.8 mm	adjustable
H	hole depth	14 mm	hidden
z_T	insertion target	10 mm	adjustable
k_n	contact stiffness	5 N/µm	adjustable
c_n	contact damping	1500 N s/m	adjustable
δ_r	damping ramp	0.25 µm	code
k_t, c_t	friction spring and damper	$k_n/2$, $c_n/2$	code
F_{dmg}	damage limit, one contact	60 N	adjustable
τ_s	wrist sensor lag	2 ms	adjustable
τ_d	force signal delay	0 ms	adjustable
σ_F	force noise, one sigma	0.15 N	adjustable
σ_x	encoder noise at the tool	0.5 µm	hidden
g	gravity	9.81 m/s^2	hidden

The stiffest contact mode, the 0.47 kg tip on 5 N/µm, rings near 3.3×10^3 rad/s, so the step resolves each period about nineteen times. Halving the step, with the control period held at 0.3 ms, changes the largest force of the angular-error case by 0.0003 % and leaves its insertion time unchanged. Every run starts with the tip at rest 3 mm above the nominal surface and the weight carried, the historian logs at 100 Hz, and generators seeded from 20261021 supply the noise and, separately, the challenge draws, so a run replays exactly.

13.3.6 Assumptions

The section is planar, with one lateral axis, the depth and one tilt. A round peg in a round hole adds a second tilt axis and contact along the rim, which changes the jamming forces by a geometric factor.

The wrist, the gripper and the peg are one rigid body pushed by the commanded wrench. Arm dynamics, joint flexibility, backlash and structural resonance are absent, although these modes between the motor and the tool are what limit force control on a real arm [9].

Contact is a penalty spring of one stiffness that lumps the part, the fixture and the peg. Penetration stays under 12 µm while every contact is below the damage limit, less than a quarter of the clearance, so the geometry is not distorted where it matters, but burrs, waviness and local yielding are not modeled.

One friction coefficient serves for sticking and sliding and it does not wear. Real surfaces often stick harder than they slide, which would add a stick-slip chatter the model does not show.

Damage is a threshold on the largest single contact force at one physics step. Real damage also depends on how long a load lasts, how often it recurs and where it lands.

The wrist sensor is perfectly tared and the fixture is rigid. The part does not move in the fixture, and the fixture moves only between insertions.

13.4 Three Controllers on One Wrench Law

Control executes on every third physics step, every $\Delta t_c = 0.3$ ms, and is handed that interval as its sample time. The structure common to the three controllers is shown in Figure 13.2.

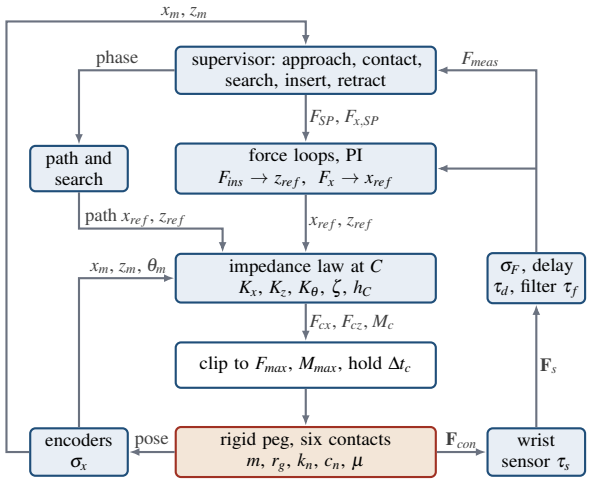


Figure 13.2 Signal flow of the controllers. The supervisor sets the phase and the force setpoints, the force loops or the programmed path write the references, and one impedance law turns them into the wrench at C. The controller reads only the encoders and the lagged, noisy and optionally delayed wrist sensor, never the contact forces.

13.4.1 The Cartesian Wrench Law

Every strategy ends in one law applied at the compliance center, as shown in Equation (13.6).

$$\begin{aligned} F_{cx} &= K_x\left(x_{ref,C} - x_C\right) + D_x\left(\dot{x}_{ref} - \dot{x}_C\right) \\ F_{cz} &= K_z\left(z_{ref,C} - z_C\right) + D_z\left(\dot{z}_{ref} - \dot{z}_C\right) - mg \\ M_c &= K_\theta\left(\theta_{ref} - \theta_m\right) - D_\theta\,\omega_m \end{aligned} \tag{13.6}$$

with $D_x = 2\zeta\sqrt{K_x m}$, $D_z = 2\zeta\sqrt{K_z m}$ and $D_\theta = 2\zeta\sqrt{K_\theta I_C}$, where $I_C = m[r_g^2 + (h_G - h_C)^2]$. The measured position of C is $x_C = x_m + h_C \sin\theta_m$ and $z_C = z_m - h_C\cos\theta_m$, the reference is carried up to C the same way from the programmed tip position, $\theta_{ref} = 0$ is the robot's vertical, and the rates of C include the $\omega_m h_C$ terms. Each axis is the impedance law of Equation (1.14), written at C. Each force is clipped to $\pm F_{max}$, the moment to $\pm M_{max}$, and all three are held for the control period. Position and force are never demanded on the same axis at once, because a force loop that owns an axis does so by writing that axis's reference.

The term $-mg$ carries the payload's weight as a force at C but not its moment about C. The weight acting $h_G - h_C$ above C therefore adds a moment $mg(h_G - h_C)\sin\theta$ in the direction of the lean, which with C at the tip is a negative rotational stiffness of $mgh_G = 1.77\,\mathrm{N\,m/rad}$. The contacts feel $K_\theta - 1.77\,\mathrm{N\,m/rad}$, which is 8.2 at the default of 10 and 1.2 at 3. Below 1.77 N m/rad the peg would be unstable when held in free space, which is why the rotational stiffness has a lower limit of 2 N m/rad, where the contacts feel 0.23 N m/rad.

13.4.2 Stiff and Impedance Programs

The controller settings are listed in Table 13.3. The stiff program is the robot's own position servo, the law of Equation (13.6) with $K_x = K_z = 200\,\mathrm{N/mm}$, $K_\theta = 500\,\mathrm{N\,m/rad}$, $\zeta = 0.7$ and C at the tip, and it follows the programmed path to the target depth without reading the force sensor. Its damping, sized for the full 2 kg, acts on a tip whose lateral effective mass is 0.47 kg, so the servo is stable only while the control period stays short. In model runs with the control period changed, a 0.1 mm step of the lateral command overshoots by 4.8 % at the executed 0.3 ms, 5.6 % at 0.5 ms and 11.8 % at 0.6 ms, and at 0.7 ms it diverges, reaching 411 % within 0.3 s. The effective mass is the cause. With

Table 13.3 Controller Settings. Level B Is Shown to a Beginner, A Only in Advanced Mode, and C Marks a Fixed Constant of the Code

Symbol	Meaning	Default	Range	L
K_x, K_z	lateral, axial stiffness	3, 5 N/mm	0.2–100, 1–50	B
K_θ	rotational stiffness	10 N m/rad	2–200	B
ζ	damping ratio	0.7	0.2–2	A
h_C	compliance center height	0 mm	0–110	A
v_{app}	approach speed	10 mm/s	1–50	B
h_{slow}	slow-down height	1 mm	0–3	B
F_{SP}, $F_{x,SP}$	force setpoints	12, 0 N	2–40, ±10	B
$K_{c,F}$, $\tau_{I,F}$	insertion loop	0.2 mm/N, 0.02 s	0–0.5, 0.005–1	B
$K_{c,x}$, $\tau_{I,x}$	lateral loop	0.03 mm/N, 0.1 s	0–0.5, 0.01–2	B
F_{lim}	overload limit	40 N	5–150	B
τ_f	force signal filter	3 ms	0–30	A
F_c, F_s	contact, search force	2, 5 N	0.5–10, 1–20	A
A	search amplitude	1 mm	0–2.5	A
n_r	retries allowed	2	0–5	A
K, K_θ	stiff servo	200 N/mm, 500 N m/rad	—	C
v_{fast}	transfer speed	50 mm/s	—	C
v_{ret}, v_{lat}	retract, lateral speed	25, 20 mm/s	—	C
$\dot{z}_{max}$	rate limit on z_{ref}	25 mm/s	—	C
T_{sw}	search period, 3 per search	0.8 s	—	C

the center of mass lowered to 50 mm above the tip, which raises that mass to 1.00 kg, the same step overshoots 6.6 % at 1 ms and 11.8 % at 1.1 ms, and it diverges only at 1.2 ms.

The impedance program follows the same path through the springs of Table 13.3 and does not read the force sensor either. Its path is programmed F_{SP}/K_z beyond the target, to 12.4 mm at the defaults, so that the axial spring pushes with the 12 N setpoint when the tip reaches 10 mm. Both programs command the reference down at v_{fast} until it is h_{slow} above the nominal surface and at v_{app} after that, with the reference speed fed forward. Both declare the insertion done when the measured tip comes within 20 µm of the target, and both give up once the reference has rested at the end of its path for 1 s.

13.4.3 The Contact-Aware Sequence

The sequence runs on the same impedance law and reads the wrist sensor. It approaches like the impedance program, with its path continuing to 13 mm, until the measured insertion force exceeds the contact threshold F_c, and it records the contact height. It then presses with the insertion loop at the search force F_s for 0.12 s, and if the peg has not dropped 0.3 mm below the contact height in that time, it searches. The search sweeps the lateral reference sinusoidally about its value at contact with a period of 0.8 s and an amplitude that grows to A over the first 1.2 s, and it ends either when the peg drops 0.3 mm or, after three periods, as a failed alignment. The insertion phase regulates the insertion force to F_{SP} and the side force to $F_{x,SP} = 0$, so that the hole centers the peg. The sequence retracts to 1 mm above the contact height at v_{ret} and tries again, up to n_r times, when the measured force magnitude exceeds F_{lim}, when the peg gains less than 0.1 mm in 0.4 s while inserting, or when a search fails, and any attempt is abandoned after 6 s.

13.4.4 The Force Loops

Both force loops use the shared velocity-form PID of Section 1.6.2, Equations (1.19) to (1.22), here with proportional and integral action only, $\tau_D = 0$. The output u of each loop is the reference it owns, sampled every Δt_c. Back-calculation acts on the integral term alone with the tracking time constant $T_t = \tau_I$, and the clamp and the rate limit apply to the emitted output, never to the running sum of the proportional increments. When a loop is not in control it tracks, with its integral set so that its output equals the reference in use, and the entry into force control is bumpless by construction.

The insertion loop has $a = +1$ and writes z_{ref} within -5 to 13 mm at no more than 25 mm/s, with $K_{c,F} = 0.2\,\mathrm{mm/N}$ and $\tau_{I,F} = 0.02\,\mathrm{s}$. It is reverse acting in the convention of Section 1.3, because a

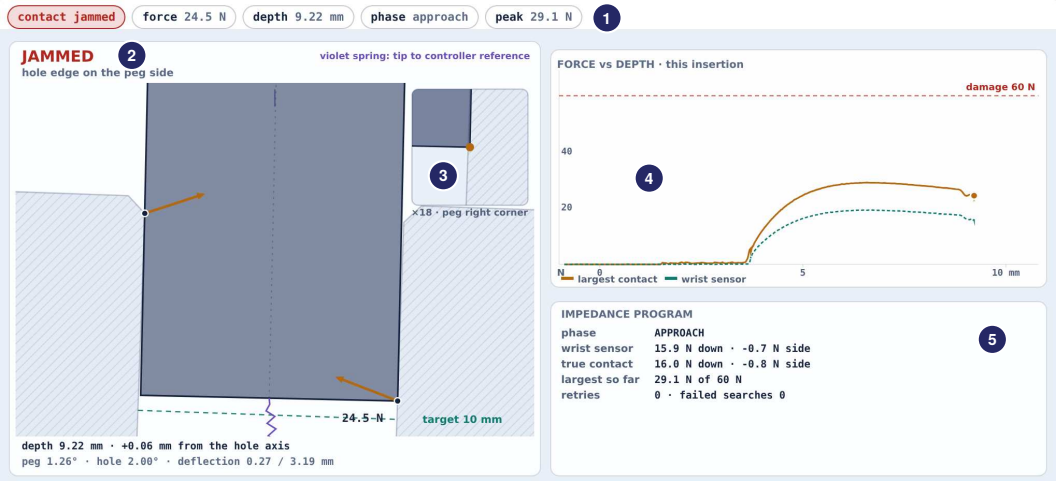


Figure 13.3 Scenario 4, Friction increase, as named in the dropdown, at $t = 2.00\,\mathrm{s}$ of a run of the impedance program with nothing changed, played at 0.25 times real speed, cropped to the plant view. The badge row (1) reads the contact jammed and a peak of 29.1 N. The cutaway (2) reads JAMMED, with force arrows at the left entry edge on the side of the peg and at the peg's right corner on the far wall, where the largest contact carries 24.5 N and the magnifier (3) looks. The zigzag spring below the peg runs 3.19 mm down to the controller's reference, and the peg leans 1.26° in a hole tilted 2.00°, 9.22 mm deep. The force against depth plot (4) rises from about 3.7 mm to a broad plateau near 29 N, with the wrist reading below it. The program panel (5) reads the insertion force at 15.9 N against 16.0 N true and a side force of –0.7 N, with the largest force so far 29.1 N of 60.

reading below the setpoint moves the reference deeper, which raises the force. The lateral loop has $a = -1$, direct acting, and writes x_{ref} within $\pm 3\,\mathrm{mm}$, with $K_{c,x} = 0.03\,\mathrm{mm/N}$ and $\tau_{I,x} = 0.1\,\mathrm{s}$, so it moves the reference in the direction of the measured side force and yields to whichever wall pushes the peg. While a force loop owns an axis, the reference speed fed forward on that axis is zero.

In manual mode the operator sets the z and x commands directly, with jogs of 0.1 and 0.05 mm, and they become the references of Equation (13.6) at the stiffness of the selected strategy while both force loops track. A jog of 0.1 mm against the part with the stiff servo is about 20 N of contact force.

Three models are kept apart. The simulation model is that of Section 13.3. The controllers carry no model of the plant beyond the payload weight, the nominal hole at $x = 0$ and $z = 0$ and the programmed target, and nothing is identified from data. The estimates of Section 13.5 are quasi-static balances and a linearized force loop that the application never uses.

13.5 What Sets the Contact Force

Four short estimates built from the constants of Tables 13.2 and 13.3 account for most of what the scenarios show, each checked against the simulator, and Figure 13.3 shows the instant the third examines.

13.5.1 Stiffness and the Chamfer

A peg whose corner lands on the chamfer $x_o - c$ outside the hole wall enters only after the chamfer has pushed it that far sideways, which costs $K_x(x_o - c)$ against the lateral spring. A corner sliding down a 45° chamfer with friction μ receives a force whose vertical part is $(1+\mu)/(1-\mu)$ times its

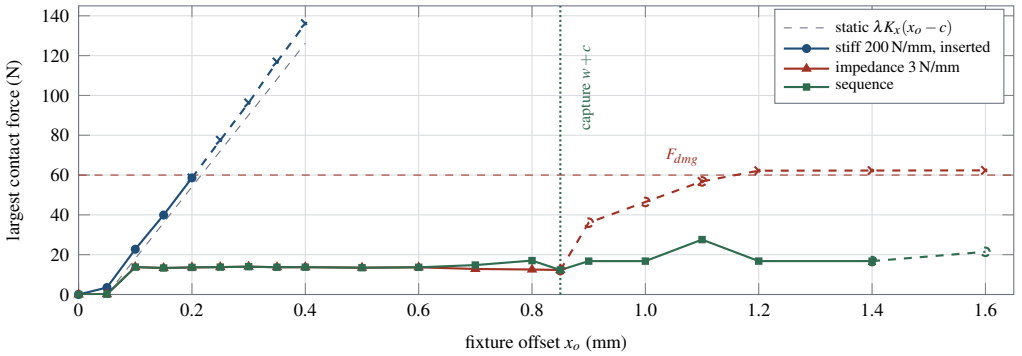


Figure 13.4 Largest contact force against fixture offset for the three controllers at their defaults, from case 2 with the offset changed. Filled circles are the stiff servo, filled triangles the impedance program and filled squares the sequence, all on solid lines while the part is inserted. On the dashed continuations, crosses are damaged parts and open circles missed holes. The thin dashed line is the static estimate. The stiff servo follows the static estimate of Equation (13.7) and passes the 60 N limit between 0.2 and 0.25 mm, the impedance program is set by the landing until the capture range ends, and the search carries the sequence to 1.4 mm.

lateral part, so the contact carries λ times the lateral force it delivers, as shown in Equation (13.7).

$$\lambda = \frac{\sqrt{(1+\mu)^2 + (1-\mu)^2}}{1-\mu} = \frac{\sqrt{2}\sqrt{1+\mu^2}}{1-\mu} \tag{13.7}$$

At $\mu = 0.2$ the factor is $\lambda = 1.80$ with a vertical to lateral ratio of 1.50, and the damage instant of case 2 matches both, with 60.5 N at the left corner of which 33.6 N is lateral and 50.3 N vertical. The stiff servo can therefore absorb only $F_{dmg}/(\lambda K_x) = 0.17$ mm of sideways correction, and it damages the part once $x_o > c + F_{dmg}/(\lambda K_x) = 0.22$ mm. In case 2 the peg meets the chamfer 0.45 mm down and is damaged 0.62 mm down, after that same correction of 0.17 mm. The measured largest force is 22.7 N at 0.1 mm, 58.6 N at 0.2 mm and 77.5 N, with the part damaged, at 0.25 mm, against the static 18.0, 54.1 and 72.1 N, and its slope between 0.1 and 0.4 mm is 378 N/mm against $\lambda K_x = 361$ N/mm, as shown in Figure 13.4. The 3 N/mm spring needs 1.05 N for the correction at 0.4 mm, so its largest force is the landing, which stays between 12.3 and 14.0 N for every offset from 0.1 mm to the capture range of $w + c = 0.85$ mm.

> **TRY IT IN THE APP** **2 · Lateral Offset**
>
> Load the case and press Run. Watch the force arrow on the chamfer and the largest contact force: the stiff servo damages the part, and the force climbs to 136.1 N before the run stops itself. Press Reset, set Controller to Impedance before pressing Run, and the same part goes in with a largest force of 13.7 N.

Pause. Try Exercise 13.1 before reading on.

13.5.2 The Landing

A landing is a moving mass stopped by the part's stiffness, and it is over in about a millisecond. The corner that meets the chamfer presents an effective mass along the chamfer normal given by Equation (13.8).

$$m_n = \left[\frac{1}{m} + \frac{(\mathbf{r}_{GP} \times \mathbf{n})^2}{m r_g^2} \right]^{-1}$$
$$F_{peak} \approx v \cos 45^\circ \sqrt{k_n m_n} \tag{13.8}$$

where $\mathbf{r}_{GP}$ runs from G to the landing corner and v is the landing speed. The corner's 0.83 kg stopped without damping by 5 N/µm gives 1.44 N per mm/s. A least-squares line through the origin fits the simulator at 1.35 N per mm/s over landing speeds from 2.9 to 59.6 mm/s, from 4.24 N at the slowest to 80.2 N at the fastest, and the first impact of the stiff servo peaks at 13.3 N from 9.9 mm/s on the same line, because nothing in any of the three controllers moves in a millisecond. In case 5 the force stays above half its 13.5 N peak for 0.7 ms, while the 2 ms sensor and the 3 ms filter pass at most 2.6 N to the controller.

🕮 **Pause.** Try Exercise 13.2 before reading on.

13.5.3 The Jam

In two-point contact the clearance forces the peg to lean $\theta = \varphi - 2c/\ell$, where $\ell = Z - w$ is its engagement below the entry edge. The moment that the rotational spring and the weight leave unbalanced, $(K_\theta - mgh_G)\theta$, has to come from the two side contacts as a couple of normal forces N about ℓ apart, and their friction, with the small vertical share of the tilted normals, resists the push of the axial spring. The peg stops at the first depth where Equation (13.9) holds.

$$\begin{aligned} 2\mu N + N(\sin\varphi - \sin\theta) &\geq K_z\left(z_{goal} - Z\right) \\ N = \frac{(K_\theta - mgh_G)\,\theta}{\ell}, \qquad \theta &= \varphi - \frac{2c}{\ell} \end{aligned} \tag{13.9}$$

where $z_{goal} = z_T + F_{SP}/K_z = 12.4$ mm is the end of the impedance path. For case 4 the balance places the jam at 9.19 mm against the 9.22 mm measured, and at μ of 0.30, 0.40 and 0.50 at 9.73, 8.61 and 7.40 mm against 9.75, 8.66 and 7.52 mm. Over a grid of 36 runs, K_θ from 3 to 20 N m/rad and μ from 0.2 to 0.8, it separates the 21 jams from the 15 insertions without an error. Its depth is within 0.43 mm for K_θ up to 10 N m/rad and within 0.92 mm at 20, where larger forces penetrate up to 9.4 µm and the peg leans 0.18° less than the clearance forces, the $2\delta/\ell$ that the penetration allows.

At the instant of Figure 13.3, 2.00 s into case 4, the balance can be read off the contacts. The peg leans 1.26° at 9.22 mm, the spring and the weight leave 0.181 N m about the tip, and over the 8.5 mm between the contacts that gives $N \approx 21.3$ N against the measured 23.1 and 21.8 N. Both sites sit on their friction cones, with tangential forces of 8.04 and 7.61 N, ratios of 0.348 and 0.349 at $\mu = 0.35$, and their friction of 15.6 N together with 0.3 N from the tilted normals balances the 15.9 N that the axial spring's 3.19 mm deflection supplies. Equation (13.9) points to two remedies the cases test, a lower friction coefficient and a softer rotational spring, and case 4 adds a third, keeping the compliance center at the tip, where the lateral spring cannot turn the peg.

🕮 **Pause.** Try Exercise 13.3 before reading on.

13.5.4 The Delay Margin of the Force Loop

While the sequence presses, the contact is a thousand times stiffer than the axial spring, so the contact force follows the reference through K_z and the loop gain is $K_{c,F}K_z$. With the sensor lag, the filter and the delay, the open loop is Equation (13.10).

$$L(s) = K_{c,F}K_z\left(1 + \frac{1}{\tau_{I,F}s}\right)\frac{\mathrm{e}^{-\tau_d s}}{(\tau_s s + 1)\left(\tau_f s + 1\right)} \tag{13.10}$$

At the default $K_{c,F} = 0.2$ mm/N the gain $K_{c,F}K_z$ is 1.0. With the contact mode and the sampling the code applies (the wrench held over each 0.3 ms period, the filter updated from the current sample and the integral carried from the previous scan) included, the crossover is 116 rad/s and the phase margin without delay is 124°, so the loop tolerates 18.7 ms of delay and would oscillate with a period of 54 ms at that limit. The margin of a purely integral force loop, Equation (1.16), does not apply here. With $K_{c,F}K_z$ at 1.0 the proportional term alone keeps the magnitude of the controller and spring at one or more at every frequency, so the sensor lag and the filter, not the integral gain, set the crossover.

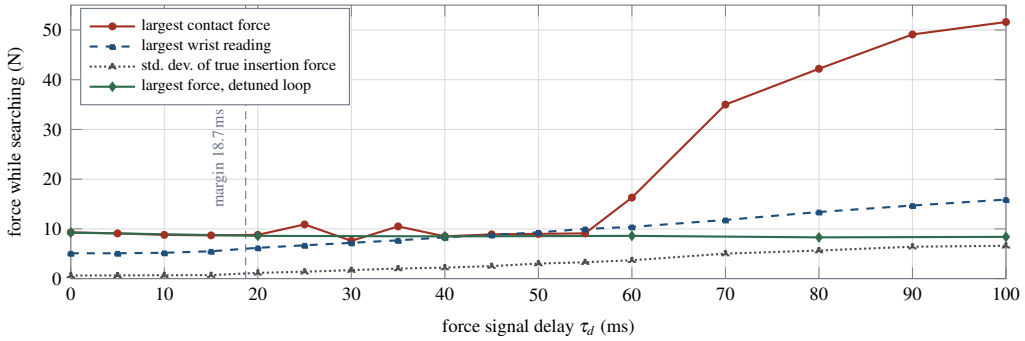


Figure 13.5 The searching press of case 7 against the force signal delay. The default loop starts to oscillate near the 18.7 ms margin of Equation (13.10), the rate limit holds the swing below the search force until about 55 ms, and beyond it the landings grow while the wrist reading stays near a third of them. Filled circles on a solid line are the largest contact force, filled squares on a dashed line the largest wrist reading, triangles on a dotted line the standard deviation of the true insertion force, and diamonds the largest force of the detuned loop, 0.1 mm/N and 0.05 s, which is unaffected.

Halving the gain to 0.1 mm/N and lengthening the integral time to 0.05 s moves the crossover to 11.5 rad/s with 117° of margin, which tolerates 177 ms.

The simulator bears the margin out. In a counterfactual run with the reference rate limit removed from a copy of the controller, the standard deviation of the true insertion force while searching rises from 0.69 N at a delay of 14 ms to 2.66 N at 19 ms, and at 20 ms the press loses contact, lifting off 19 times and landing at up to 43.1 N. As shipped, the 25 mm/s limit on z_{ref} bounds the same oscillation. It starts at the same delay, 0.70 N at 15 ms and 1.16 N at 20 ms with a period of 58 ms, and grows only as fast as the limit lets the reference swing, to 3.03 N at 50 ms. Lift-offs begin at 55 ms, where the swing exceeds the 5 N search force, and at 80 ms the landings reach 42.2 N while the largest reading is 13.4 N, as shown in Figure 13.5. The detuned loop holds the deviation between 0.62 and 0.71 N, and the peg in contact 99 % of the time, out to 100 ms. A delay inside the loop also sets the chatter boundary of the milling cut in Volume 7, Chapter 13, where each tooth cuts the surface the previous tooth left.

Table 13.4 Scenarios and Their Presets

#	Scenario	Preset
1	Perfect alignment	stiff servo
2	Lateral offset	stiff servo, $x_o = 0.4$ mm
3	Angular error	impedance, $\varphi = 2°$
4	Friction increase	as case 3, $\mu = 0.35$
5	Fragile component	impedance, $x_o = 0.5$ mm, $F_{dmg} = 10$ N
6	Excessive stiffness	impedance, $x_o = 0.5$ mm, $K_x = 40$ N/mm
7	Delayed force signal	sequence, $x_o = 1.2$ mm, $\tau_d = 80$ ms
8	Early contact	sequence, $\Delta h = 2$ mm, $x_o = 0.3$ mm
C	Challenge	stiff servo, 100 parts, $\mu = 0.35$, offsets within ± 1.2 mm and tilts within $\pm 2°$

Table 13.5 Measured Results. Forces Are the Largest Single Contact Force

Case and setting	Measured
1, aligned	in at 1.14 s, no contact
1, x_o 0.1 / 0.2 / 0.3 mm	22.7 / 58.6 N / damaged, 96.3 N
2, stiff	damaged at 0.223 s, 136.1 N
2, impedance / sequence	13.7 N, in at 1.14 / 0.63 s
2, 1.2 mm, impedance / sequence	damaged, 62.2 N / in, 1.59 s
2, 1.2 mm, sequence, $K_x = 1$ N/mm	missed, 2 failed searches
3, $K_\theta = 10$	in at 1.33 s, 27.8 N, 1.32°
3, $K_\theta = 50$ / stiff	damaged 4.86 / 4.25 mm in, 67.1 / 117.2 N
4, $K_\theta = 10$	stuck at 9.22 mm, 29.1 N
4, K_θ 3 / 5	in at 1.20 / 1.28 s, 10.3 / 14.7 N
4, $h_C = 110$ mm	stuck at 4.96 mm, 56.3 N
5, v_{app} 10 / 7 / 5 / 3 mm/s	13.5 (damaged) / 9.4 / 7.0 / 4.2 N
5, insertion time at 7 / 5 / 3 mm/s	1.62 / 2.25 / 3.72 s
6, K_x 40 / 20 / 10 N/mm	96.7 (damaged) / 18.3 / 13.5 N
7, $\tau_d = 80$ ms	42.2 N true, 13.4 N read, 60 % in contact
7, 80 ms, 0.1 mm/N, 0.05 s	8.3 N, 99 %, in at 1.72 s
7, $\tau_d = 0$	9.3 N, 99 %, in at 1.59 s
8, as loaded	damaged at 38 ms, 80.2 N
8, $h_{slow} = 2.5$ mm	12.5 N, in at 0.63 s
C, stiff / impedance / sequence	5 / 66 / 87 of 100 inserted
C, sequence, $K_\theta = 3$	100 of 100, 30.2 N, 157.9 s

TRY IT IN THE APP **7 · Delayed Force Signal**

Press Run and watch both traces of the force-versus-depth plot while the sequence presses and searches. The landings reach 42.2 N while the wrist reading never passes 13.4 N. Press Reset, set Force loop gain to 0.1 mm/N and Force loop integral time to 0.05 s before pressing Run, and the press stays in contact 99 % of the time.

13.6 Scenarios and Measured Results

Table 13.4 lists the cases, which build from case 1 to the challenge, with the preset each loads. Each case is credited, as Section 1.6.4 describes, when the learner makes the attempts its briefing names, with every attempt judged at its end, whether the part is inserted, stuck, missed or damaged. The challenge is judged on the case as given, and changing a model parameter or a disturbance, or firing an extra disturbance button, voids the attempt. The values of Table 13.5 were read from headless runs of the shipped application at its default seed, with the scenario loaded as shipped and any named change made before the run. Figure 13.6 draws the largest contact forces of that table as bars.

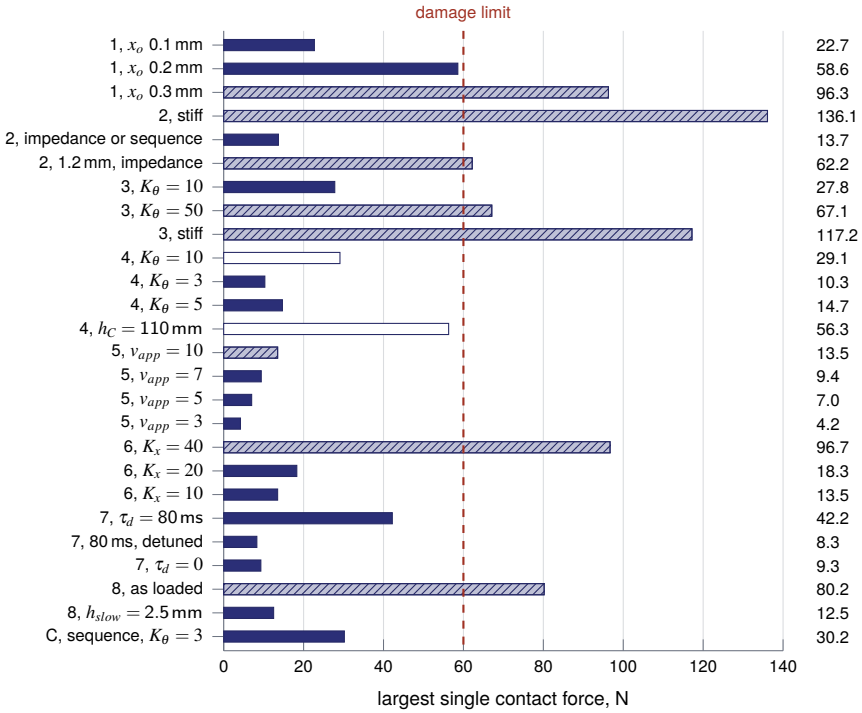


Figure 13.6 The largest contact forces of Table 13.5 drawn as bars, by case and setting (K_θ in N m/rad, K_x in N/mm, v_{app} in mm/s). Hatched bars damaged the part, open bars left it stuck, and solid bars did neither. The dashed line is the 60 N damage limit, and the part of case 5 cracks above 10 N. Notice that every case has a setting whose bar ends far left of the line, and that the bars past it belong to stiff settings, to the fast landing of case 8 and to a hole beyond the chamfer's reach.

13.6.1 Position Control and Its Tolerance

Aligned, the stiff servo puts the peg in at 1.14 s without touching the part, and shifted 0.3 mm it damages the part 0.72 mm down the chamfer as the force reaches 96.3 N. Case 2 sets the offset at 0.4 mm. The part is damaged 0.223 s into the run, and the force keeps climbing to 136.1 N before the run stops. The impedance program inserts the same part at 1.14 s with 13.7 N, and the sequence at 0.63 s, because it detects the contact and regulates the insertion force instead of creeping down at the approach speed. Below 0.35 mm the sequence never reads more than its 2 N threshold, keeps to the path and takes the same 1.14 s.

Beyond the capture range the order reverses. At 1.2 mm the impedance program keeps pushing on the top face until the peg cocks 2.2° onto the edge of the chamfer and the part is damaged at 62.2 N, while the sequence detects the contact, sweeps until the peg drops into the chamfer and inserts it at 1.59 s with 16.8 N. The search reaches offsets of 1.4 mm and misses at 1.6 mm. A lateral spring of 1 N/mm is too soft to search, because the 1 N of friction under the 5 N search force takes a millimeter of deflection, the whole amplitude, and the sequence gives up after two failed searches at the 6 s attempt limit.

13.6.2 Tilt, Friction and the Rotational Spring

Case 3 tilts the fixture 2°. At 10 N m/rad the contacts turn the peg, and it reaches the target at 1.33 s with 27.8 N, leaning 1.32° in the 2.00° hole. The diametral clearance of 0.1 mm over the 9.2 mm between the entry edge and the tip allows 0.62° of the 0.68° difference, and contact penetrations of up to 5.4 µm take up the rest. At 50 N m/rad the same turn leaves 5.9 times the unbalanced moment

for the contacts to supply, and the part is damaged 4.86 mm in with 67.1 N, and the stiff servo, at 500 N m/rad, damages it 4.25 mm in with 117.2 N.

Case 4 dries the parts to $\mu = 0.35$ and changes nothing else. The right corner first meets the tilted wall 1.54 mm down, the second contact forms at 3.7 mm, and the largest force peaks at 29.1 N at 6.6 mm before easing toward the jam at 9.22 mm. The impedance reference reaches the end of its path at 1.38 s, the scene reads JAMMED from 1.80 s, and the program gives up at 2.38 s. At 3 N m/rad the peg goes in at 1.20 s with 10.3 N, and at 5 N m/rad with 14.7 N, while moving the compliance center to the wrist, 110 mm up, jams it at 4.96 mm with 56.3 N.

> ⚠ **OPEN CHALLENGE** **Built-In Compliance or Programmed Compliance**
>
> A cell can take up position error with a mechanism, such as a compliant wrist, or with an active compliant controller. Large position or force uncertainties can be accommodated by the controller, while smaller ones can be removed by making the mechanism more compliant. When to tune the controller and when to change the mechanism is still an open question of peg-in-hole research [19]. Progress would be a design rule that splits a cell's tolerance budget between the hardware and the control law before either is built.

13.6.3 The Force Budget

Case 5 lands the impedance program 0.5 mm off on a part whose latch cracks above 10 N. At the default 10 mm/s the landing reaches 13.5 N and cracks it 0.35 mm down the chamfer on the first step over the limit, while the controller's reading never exceeds 2.6 N. The peak falls in proportion to the speed, to 9.4 N at 7 mm/s, 7.0 N at 5 mm/s and 4.2 N at 3 mm/s, and the insertion time rises to 1.62, 2.25 and 3.72 s, so the force budget rather than the geometry sets the cycle time. Case 6 raises the lateral stiffness to 40 N/mm at the same offset. The spring pulls the peg back toward the programmed x against the hole's left wall as it enters, the contact forces turn it, and 5.15 mm in it leans 1.57° with its left corner digging into the wall past the limit. The largest force reaches 96.7 N before the peg reaches the target. At 20 N/mm the peak is 18.3 N and at 10 N/mm it is 13.5 N, which is the landing itself.

13.6.4 A Late Signal and an Early Contact

Case 7 gives the sequence a hole 1.2 mm off, so that it must press on the top face and search, and delays the force signal by 80 ms. With no delay the press keeps at least one site loaded above 0.05 N, the count the application logs, 99 % of the searching time, its largest force is 9.3 N, and the part is in at 1.59 s. With the delay the loop oscillates as Section 13.5 predicts. The peg is in contact only 60 % of the searching time and lifts off 12 times, the landings reach 42.2 N, and the controller's reading never passes 13.4 N, so the 40 N overload never trips. The part still goes in at 1.72 s, only because 42.2 N is under this part's limit. Detuned to 0.1 mm/N and 0.05 s, the same delay leaves the press in contact 99 % of the time with 8.3 N, and the part is in at 1.72 s.

Case 8 raises the part 2 mm, with an offset of 0.3 mm that the chamfer can catch. The slow-down still begins 1 mm above the nominal surface, so the peg meets the chamfer 38 ms into the run at 59.6 mm/s, faster than the 50 mm/s transfer because the damped spring overshoots in speed while the tool catches up with its reference. The first step over the limit carries 70.0 N, the peak is 80.2 N, and the wrist sensor has registered 7.4 N by the time the run stops. Detecting contact cannot help, because the impact is over before the signal arrives, and the impedance program, which reads no sensor at all, is damaged at the same 80.2 N. A slow-down height of 2.5 mm lands the peg at 9.5 mm/s with 12.5 N, and the part is in at 0.63 s.

13.6.5 One Hundred Parts

The challenge loads 100 parts in a row, each in a fixture with its own offset within ±1.2 mm and tilt within ±2°, on dry parts at $\mu = 0.35$, and it is met when at least 95 are inserted with no damage event. The shipped stiff program inserts 5, damages 93 and jams 2, with a largest contact force of 69.4 N, 90

parts short of the target, and the set ends after 58.2 s. The impedance program at its defaults inserts 66, with 21 missing holes beyond the capture range, 8 jammed and 5 damaged. The sequence at its defaults inserts 87, and the 13 that jam all have tilts of 1.71° or more, while every tilt it inserts is 1.69° or less, and its 36 retries repeat the motion without curing them. With $K_\theta = 3\,\mathrm{N\,m/rad}$ the sequence inserts all 100 with no damage event and no retry, with a largest contact force of 30.2 N over the whole set and a mean insertion time of 1.01 s, and the set takes 157.9 s. The last part is done at 157.7 s, and the run pauses 0.2 s later.

The four tallies are scored on the same 100 parts: the part draws come from a random stream of their own, seeded from the scenario, so the sensor noise an attempt consumes cannot change the next part. Over ten further seeds, with the four configurations again meeting the same parts on each, the stiff program inserts 2 to 6, the impedance program 59 to 70, the default sequence 80 to 88, and the suggested configuration 100 on every seed with no damage and a largest force of 28.3 to 30.1 N.

> ✦ DID YOU KNOW? **The Most Precise Program Scores Worst**
>
> From the simulator: on the same 100 parts of the challenge, the stiff servo inserts 5, the impedance program 66 and the contact-aware sequence 87. The sequence with a rotational spring of 3 N m/rad inserts all 100 (Table 13.5).

13.7 Technology in Practice

The cell of Section 13.3 reads a wrist force sensor and the joint encoders, and it moves the peg through one wrench law. Figure 13.7 draws its loops with real devices in the place of the schematic's symbols.

What Measures It

Force-based robotic assembly exists in industry mainly as force and torque sensors at the end of the arm, sold by robot makers and integrators, often with no performance specification beyond the sensing itself [11]. Sensors that read the deformation of a compliant body with strain gauges, with capacitive electrodes or with optical fibers have all been developed [20]. The wrist sensor of Section 13.3, a 2 ms lag with 0.15 N of noise ahead of the controller's 3 ms filter, stands for such a sensor, and the encoders with 0.5 µm of noise stand for the joint encoders of the arm.

> ⏲ TECHNOLOGY **Sensor: Six-Axis Wrist Force Sensor**
>
> Force-based assembly cells mostly sense contact with a force and torque sensor at the end of the arm [11]. A conventional six-axis sensor measures three forces and three moments from the deformation of a single compliant structure. Strain gauges read that deformation with high accuracy, but they are sensitive to electromagnetic interference and often show cross-axis coupling, in which a load in one direction appears in the others [20]. On a trend, coupling shows as a side force that rises and falls with the push. An offset left in the reading makes the arm jerk when it switches from position to force control [10]. The model's sensor, perfectly tared, has neither fault.

What Moves It

The robot's own position loops do most of the work. Force loops closed around them see a plant that the position loops have decoupled and linearized, and the role of a passive compliance in the speed of the task and in its rejection of disturbances has been analyzed [12]. Impedance control is typically used for fast contact tasks such as polishing, metal removal and some assemblies [10]. The clipped wrench of Equation (13.6), held over each control period, stands for the arm's drives.

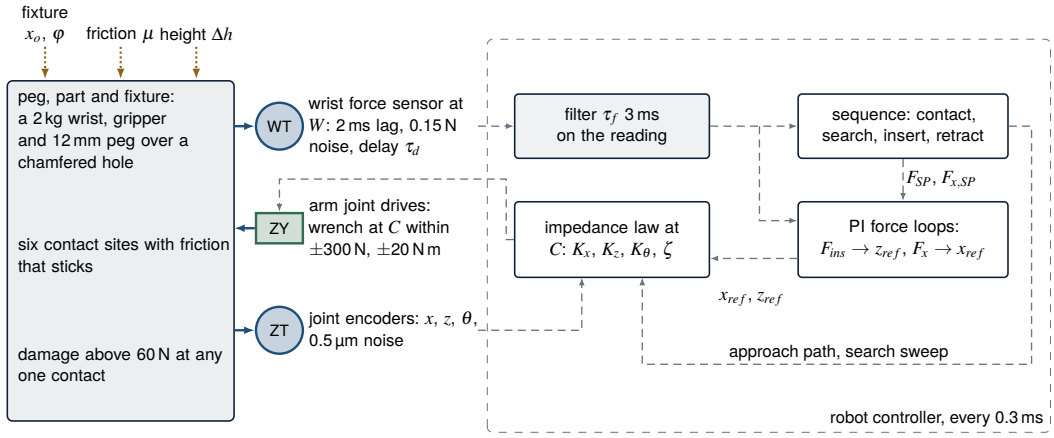


Figure 13.7 The insertion loops of the chapter with real devices in place of the schematic's symbols. The wrist force sensor WT and the joint encoders ZT feed a robot controller that runs every 0.3 ms. The sequence sets the force setpoints, the PI force loops write the references, and one impedance law at the compliance center C turns them into the wrench the arm's joint drives ZY apply. Notice that the arm itself is the final element, and that every force the controller acts on passes through the sensor's lag and the filter first.

> **TECHNOLOGY** **Final Element: The Arm as a Programmable Spring**
>
> The final element is the arm itself, driven by its joint servos. Active stiffness control turns the robot into a programmable spring, where a passive tool would carry real springs and dampers in line with the gripper. Some arms infer the applied force from the torques or the currents at each joint instead of reading a wrist sensor [10], and arms built to work beside people resolve the force at the tool from torque sensors in the joints [11]. A badly damped arm resonates, and on a trend it hops along the approach direction instead of settling [10]. The wrench law of Equation (13.6) stands for these drives.

Where the Controller Runs

In discrete manufacturing a supervisor for each cell may coordinate a machine controller and a robot controller, and supervisory and lower-level loops run with cycle times from milliseconds to minutes [21]. The controllers of this chapter act every 0.3 ms, at the fast end of that range. In a real cell the impedance law and the two force loops would sit in the robot controller, beside its position servos, and the contact-aware sequence in the robot's program. That sequence is an event-based search strategy, which moves the peg around the expected hole, randomly or in a raster or a spiral, until the peg can be pushed in [10]. The sequence of this chapter sweeps a sinusoid.

> **IN PRACTICE** **Testing Force Control Against a Load Cell**
>
> A force-controlled cell is tested against an independent load cell, not the robot's own sensor, whose reading carries its own accuracy, latency and tooling offsets [10]. In one NIST test method the robot steps to a target force from free space, 32 times in each direction tested. The peak overshoot, which indicates the impact force, the settling time and the steady-state error are recorded. Assembly itself is judged by its success rate, its time and the largest and average force applied to the parts [11]. The simulator draws the true contact force beside the reading in the same spirit.

What Is Modernizing It

Arms built to work beside people now carry torque sensors in their joints and resolve the force at the tool from them, which lets them both assemble by force and react to a collision with a person [11].

Cameras join the force sensor: vision gives the hole's position from afar but is blocked in narrow spaces, so one strategy fuses images, the measured contact force and the joint positions by Bayesian probability, which needs no large training set, and judges the result by force and position together [22]. Learning methods form the third development. Strategies learned from human demonstrations and from interaction with the environment by reinforcement learning are being compared with the contact models and compliant control that this chapter uses [19]. Test methods with independent load cells and standard artifacts, including a peg-in-hole artifact, are meant to help users select a robot for force-based work [11].

13.8 Limitations

The numbers are the simulator's own design choices, a 60 N damage limit, a 5 N/µm contact and a 2 kg end effector, and no claim about a real cell's forces, cycle time or yield can rest on them. The model is planar, with one rigid body and no arm dynamics, and the assumptions of Section 13.3.6 state where each simplification breaks.

A single physics step over the limit counts as damage, so an impact of 0.1 ms weighs the same as a sustained press. Retries repeat the motion that failed, which is why the 13 jams of the default sequence in the challenge survive 36 retries. The weight's moment about the compliance center is not compensated, which makes the rotational stiffness the contacts feel 1.77 N m/rad lower than the slider reads. The loop tiles of the scorecard score the insertion force against a setpoint of zero whenever no force loop is in control, so for the stiff and impedance programs they integrate the force the sensor reported rather than a regulation error. Robot safety functions and their certification are outside what the simulation claims to represent.

> ⚠ **OPEN CHALLENGE** **Fast or Reliable, Rarely Both**
>
> Force control has been researched for decades, yet industry has been slow to adopt it for assembly. The time to implement it and a steep learning curve weigh against it, and reliable solutions are not fast, while fast solutions are not reliable. A robot can be programmed to be an expert at one assembly, but generalizing that expertise across assemblies is difficult [10]. Learned strategies promise to generalize, but their low sample efficiency still limits them on real robots [19]. Progress would be a cell that inserts a new part quickly and reliably without being tuned for it.

13.9 Conclusion

This chapter studied a robotic peg-in-hole simulator in which the moment of contact changes what the controller can command. A planar 2 kg end effector carries a 12 mm peg into a hole with 50 µm of clearance per side, through six penalty contacts whose friction sticks and a wrist sensor the controller reads only after its lag. The robot's 200 N/mm servo tolerates a fixture offset of about 0.22 mm, as the chamfer factor of 1.80 predicts, and damages the part at 0.4 mm with the force reaching 136.1 N, while a 3 N/mm spring inserts it at 13.7 N. Landings cost 1.35 N per mm/s of landing speed whatever the controller, from 4.2 N at 3 mm/s to 80.2 N for a part met during the transfer. A 2° hole on dry parts jams 9.22 mm deep, where a moment balance predicts 9.19, and inserts at 10.3 N once the rotational stiffness drops to 3 N m/rad. The force loop loses its phase margin at 18.7 ms of delay, its rate limit postpones lift-off to 55 ms, and at 80 ms it hammers the part at 42.2 N while its reading stays under 13.4 N. Across 100 seeded parts the stiff program inserts 5 and the sequence with a soft wrist inserts 100 with a largest force of 30.2 N, and 100 on each of ten further seeds. The model omits arm dynamics, the second tilt axis and duration-dependent damage. A fuller model would add a round peg, adaptive retries and a damage-energy criterion. Within those limits the simulator lets each failure of control through a contact transition be met alone and measured.

KEY POINTS

- Once the peg touches the part, a stiff robot turns every small position error into force.
- The 200 N/mm servo tolerates a fixture offset of about 0.22 mm, while a 3 N/mm spring inserts the part shifted 0.4 mm at 13.7 N.
- A landing is over within a millisecond, before any feedback can act, so the speed at contact sets its force.
- A tilted peg on dry parts jams where a moment balance predicts, and a softer rotational spring frees it.
- With a delayed force signal the press hammers the part while the controller's reading stays calm.

Where else this applies. A delay inside the loop also sets the chatter boundary of the milling cut in Volume 7, Chapter 13, and Chapter 14 closes a force loop on tissue.

References

[1] D. E. Whitney, "Quasi-static assembly of compliantly supported rigid parts," *Journal of Dynamic Systems, Measurement, and Control*, vol. 104, no. 1, pp. 65–77, 1982.

[2] ——, "Historical perspective and state of the art in robot force control," *The International Journal of Robotics Research*, vol. 6, no. 1, pp. 3–14, 1987.

[3] M. T. Mason, "Compliance and force control for computer controlled manipulators," *IEEE Transactions on Systems, Man, and Cybernetics*, vol. 11, no. 6, pp. 418–432, 1981.

[4] M. H. Raibert and J. J. Craig, "Hybrid position/force control of manipulators," *Journal of Dynamic Systems, Measurement, and Control*, vol. 103, no. 2, pp. 126–133, 1981.

[5] N. Hogan, "Impedance control: An approach to manipulation: Part I—theory," *Journal of Dynamic Systems, Measurement, and Control*, vol. 107, no. 1, pp. 1–7, 1985.

[6] L. Villani and J. De Schutter, "Force control," in *Springer Handbook of Robotics*, B. Siciliano and O. Khatib, Eds. Cham: Springer International Publishing, 2016, pp. 195–220.

[7] S. Haddadin, A. Albu-Schäffer, and G. Hirzinger, "Requirements for safe robots: Measurements, analysis and new insights," *The International Journal of Robotics Research*, vol. 28, no. 11–12, pp. 1507–1527, 2009.

[8] D. E. Whitney, "Force feedback control of manipulator fine motions," *Journal of Dynamic Systems, Measurement, and Control*, vol. 99, no. 2, pp. 91–97, 1977.

[9] S. Eppinger and W. Seering, "Introduction to dynamic models for robot force control," *IEEE Control Systems Magazine*, vol. 7, no. 2, pp. 48–52, 1987.

[10] J. Marvel and J. Falco, "Best practices and performance metrics using force control for robotic assembly," National Institute of Standards and Technology, Gaithersburg, MD, NIST Interagency/Internal Report 7901, 2012.

[11] J. Falco, J. Marvel, R. Norcross, and K. Van Wyk, "Benchmarking robot force control capabilities: Experimental results," National Institute of Standards and Technology, NIST IR 8097, 2016.

[12] J. De Schutter and H. Van Brussel, "Compliant robot motion II. A control approach based on external control loops," *The International Journal of Robotics Research*, vol. 7, no. 4, pp. 18–33, 1988.

[13] R. Volpe and P. Khosla, "A theoretical and experimental investigation of explicit force control strategies for manipulators," *IEEE Transactions on Automatic Control*, vol. 38, no. 11, pp. 1634–1650, 1993.

[14] S. R. Chhatpar and M. S. Branicky, "Search strategies for peg-in-hole assemblies with position uncertainty," in *Proceedings 2001 IEEE/RSJ International Conference on Intelligent Robots and Systems*, vol. 3. Maui, HI, USA: IEEE, 2001, pp. 1465–1470.

[15] K. H. Hunt and F. R. E. Crossley, "Coefficient of restitution interpreted as damping in vibroimpact," *Journal of Applied Mechanics*, vol. 42, no. 2, pp. 440–445, 1975.

[16] G. Gilardi and I. Sharf, "Literature survey of contact dynamics modelling," *Mechanism and Machine Theory*, vol. 37, no. 10, pp. 1213–1239, 2002.

[17] D. Karnopp, "Computer simulation of stick-slip friction in mechanical dynamic systems," *Journal of Dynamic Systems, Measurement, and Control*, vol. 107, no. 1, pp. 100–103, 1985.

[18] P. Dupont, V. Hayward, B. Armstrong, and F. Altpeter, "Single state elastoplastic friction models," *IEEE Transactions on Automatic Control*, vol. 47, no. 5, pp. 787–792, 2002.

[19] J. Xu, Z. Hou, Z. Liu, and H. Qiao, "Compare contact model-based control and contact model-free learning: A survey of robotic peg-in-hole assembly strategies," arXiv preprint arXiv:1904.05240, 2019.

[20] S. Y. Lee, J. Y. Sim, D.-Y. Seok, Y. B. Kim, J. Shim, U. Kim, and H. R. Choi, "A redundant-sensing-based six-axis force/torque sensor enabling compactness and high sensitivity," *Sensors*, vol. 26, no. 3, p. 871, 2026.

[21] K. Stouffer, M. Pease, C. Tang, T. Zimmerman, V. Pillitteri, S. Lightman, A. Hahn, S. Saravia, A. Sherule, and M. Thompson, "Guide to operational technology (OT) security," National Institute of Standards and Technology, Gaithersburg, MD, Special Publication 800-82r3, 2023.

[22] L. Qin, H. Wang, Y. Yuan, and S. Qin, "Multi-sensor perception strategy to enhance autonomy of robotic operation for uncertain peg-in-hole task," *Sensors*, vol. 21, no. 11, p. 3818, 2021.

13.10 Exercises

13.1 Concept check · 2 min

In scenario 2 the fixture sits 0.4 mm from where the program aims. The stiff servo damages the part with a contact force that climbs to 136.1 N, while the impedance program with its 3 N/mm lateral spring inserts the same peg with a largest force of 13.7 N. Which statement explains the difference?

(a) The chamfer must push the peg sideways by the offset less the clearance, and that costs force in proportion to the lateral stiffness

(b) The impedance program reads the wrist sensor and slows its approach as soon as the contact force starts to rise

(c) The stiff servo approaches the part faster, so its landing on the chamfer is harder than that of the impedance program

(d) The stiff servo's damping is sized for the full mass, so its loop becomes unstable once the peg touches the chamfer

13.2 Concept check · 2 min

In scenario 8 the part is 2 mm taller than programmed, and the contact sequence, which reads the wrist sensor and retracts above its force limit, damages it at 80.2 N. A learner lowers the force limit from 40 to 5 N before Run, and the part is damaged at the same force. Why?

(a) The force limit is checked only while the force loop inserts, and this contact arrives during the approach

(b) The impact is over in about a millisecond, while the sensor lag and the filter pass only a few newtons in that time

(c) The landing force is set by the lateral spring, and lowering the force limit leaves that spring unchanged

(d) The damage limit in this scenario is 10 N, below the force of any landing the program can make

13.3 Concept check · 1 min

In scenario 4 the impedance program jams a peg 9.22 mm deep in a hole tilted 2° on dry parts ($\mu = 0.35$). Which single change, made before Run, lets it insert the peg?

(a) Lower the approach speed to 3 mm/s, so the peg enters the tilted hole more gently

(b) Raise the rotational stiffness to 50 N m/rad, so the peg is held straighter in the hole

(c) Lower the rotational stiffness to 3 N m/rad, so the contacts need a smaller moment to turn the peg

(d) Move the compliance center to the wrist, 110 mm above the tip, as on a passive wrist

13.4 Theory and calculation · 6 min

The stiff servo holds the tip with $K_x = 200\,\mathrm{N/mm}$. The clearance is $c = 50\,\mu\mathrm{m}$ per side, the chamfer is at 45°, and a single contact above $F_{dmg} = 60\,\mathrm{N}$ damages the part.

(a) For $\mu = 0.20$, find the chamfer factor λ of Equation (13.7) and the ratio of the vertical to the lateral force on the corner. *Checkpoint:* $\lambda = 1.80$ and 1.50.

(b) Find the largest sideways correction the servo can make before the contact passes the damage limit, and the fixture offset at which that happens. *Checkpoint:* 0.17 mm and 0.22 mm.

(c) Repeat (b) for the dry parts of the challenge, $\mu = 0.35$, and find the lateral force the 3 N/mm impedance spring needs at an offset of 0.4 mm. *Checkpoint:* $\lambda = 2.31$, an offset of 0.18 mm, and 1.05 N.

13.5 Theory and calculation · 6 min

The end effector has $m = 2\,\text{kg}$, a radius of gyration $r_g = 50\,\text{mm}$ about its center of mass G, which lies $h_G = 90\,\text{mm}$ above the tip, and the contact stiffness is $k_n = 5\,\text{N}/\mu\text{m}$. The peg's corner is $a = 6\,\text{mm}$ from the peg axis and lands on a 45° chamfer whose normal points up and toward the hole.

(a) Find the effective lateral mass the tip presents to a sudden sideways push. *Checkpoint:* 0.47 kg.

(b) The lever arm of the chamfer normal about G is $(h_G - a)/\sqrt{2}$. Find the effective mass m_n of Equation (13.8) and the landing force per unit of approach speed. *Checkpoint:* 0.83 kg and 1.44 N per mm/s.

(c) The part of scenario 5 cracks above 10 N. Find the fastest safe approach speed from (b) and from the slope of 1.35 N per mm/s that the chapter fits to the simulator. *Checkpoint:* 6.9 mm/s and 7.4 mm/s.

13.6 Theory and calculation · 7 min

Scenario 4 tilts the hole $\varphi = 2°$, with clearance $c = 50\,\mu\text{m}$ per side, a chamfer of $w = 0.8\,\text{mm}$, $\mu = 0.35$, $K_z = 5\,\text{N}/\text{mm}$, $K_\theta = 10\,\text{N m}/\text{rad}$, $mgh_G = 1.77\,\text{N m}/\text{rad}$ and the end of the impedance path at $z_{goal} = 12.4\,\text{mm}$. Use Equation (13.9).

(a) At the depth $Z = 9.22\,\text{mm}$, find the engagement ℓ and the lean θ that the clearance forces. *Checkpoint:* $\ell = 8.42\,\text{mm}$ and $\theta = 1.32°$.

(b) Find the normal force N, the resisting force and the push of the axial spring, and say whether the peg stops there. *Checkpoint:* $N = 22.5\,\text{N}$, 16.0 N against 15.9 N, so it stops.

(c) Repeat (b) with $K_\theta = 3\,\text{N m}/\text{rad}$. *Checkpoint:* $N = 3.4\,\text{N}$, 2.4 N against 15.9 N, so it does not.

13.7 App challenge · 8 min

Load scenario 2, Lateral offset, which loads the stiff servo with the fixture 0.4 mm off. Use the default seed and let each run stop itself.

(a) Run the scenario as shipped. Read the Peak contact force and Damage events tiles, and the time of damage from the note. *Checkpoint:* 136.1 N, one damage event, at 0.223 s.

(b) Press Reset, set Controller to Impedance and run again. Read the Peak contact force and Insertion time tiles. *Checkpoint:* 13.7 N and 1.14 s.

(c) Press Reset, set Controller to Sequence and run again. Read the same tiles, and say why this run is faster. *Checkpoint:* 13.7 N and 0.63 s.

13.8 App challenge · 8 min

Load scenario 4, Friction increase. Use the default seed and let each run stop itself.

(a) Run the scenario as shipped. Read the depth at which the note reports the peg stuck, the Peak contact force tile, and from the exported CSV file the first time at which the column `contact_state` reads `JAMMED`. *Checkpoint:* 9.22 mm, 29.1 N, 1.81 s.

(b) Press Reset, set Rotational stiffness to 3 and run again. Read the Insertion time and Peak contact force tiles. *Checkpoint:* 1.20 s and 10.3 N.

(c) Press Reset, set Rotational stiffness to 5 and run again. Compare the three runs with the jam balance of Equation (13.9). *Checkpoint:* 1.28 s and 14.7 N.

13.9 App challenge · 8 min

Load scenario 7, Delayed force signal, in which the sequence presses and searches on a hole 1.2 mm off while its force reading arrives 80 ms late. Use the default seed, let each run stop itself and export the CSV file after each.

(a) Run the scenario as shipped. Read the Peak contact force, Insertion time and Retries tiles. In the file, find the largest value of `Fins_meas_N`, the reading the controller acts on. *Checkpoint:* 42.2 N, 1.72 s, 0 retries, and 13.3 N within 0.2 N.

(b) Press Reset, set Force loop gain to 0.1 mm/N and Force loop integral time to 0.05 s, and run again. Read the Peak contact force tile, and in the file the largest `contact_peak_N` over the rows whose `phase` reads `SEARCH`. *Checkpoint:* 16.8 N on the tile and 8.3 N while searching.

(c) Reload the scenario with the reload button, open Show Model, set Force signal delay to 0 ms and run again. Read the Insertion time tile. *Checkpoint:* 1.59 s.

13.10 Application area · 4 min

A cell engineer reviews the guarded move of scenario 8. The parts may stand up to 2 mm taller than programmed, the transfer runs at 50 mm/s, the approach at 10 mm/s, and a single contact above 60 N damages the part. Use the landing slope of 1.35 N per mm/s that the chapter fits to the simulator.

(a) Find the highest landing speed under the damage limit, and say whether any slow-down height below the height error can be made safe by a faster controller. *Checkpoint:* About 44 mm/s. No.

(b) The slow-down height is raised from 1 to 2.5 mm. Estimate the extra time per part when the part is at its nominal height, ignoring acceleration. *Checkpoint:* About 0.12 s.

13.11 Application area · 3 min

A supplier offers a passive compliant wrist whose center of compliance lies at its mounting flange, about 110 mm above the peg tip. The parts are those of scenario 4. What does the chapter predict for this wrist, where should the compliance center be instead, and which assumption of the model must be checked before the result is trusted for a round peg?

13.12 Review the agent · 5 min

An AI assistant is asked whether the insertion force loop of the sequence tolerates a 25 ms fieldbus delay and replies as follows. “The force follows the reference through the 5 N/mm axial spring, so the loop is an integrator of gain $g = K_z K_{c,F}/\tau_{I,F} = 5 \times 0.2/0.02 = 50\,\mathrm{s}^{-1}$. Its delay margin is $\pi/(2g) = 31$ ms, so the shipped tuning is safe up to about 30 ms and the 25 ms link needs no retuning.” Find the flaw and say how you would check it.